Bioactive Materials 22 (2023) 453–465

Contents lists available at ScienceDirect

Bioactive Materials

journal homepage: www.keaipublishing.com/en/journals/bioactive-materials

Injectable bone marrow microniches by co-culture of HSPCs with MSCs in 3D microscaffolds promote hematopoietic reconstitution from acute lethal radiation

Haiwei Liang [a], Yanxiao Ao [a], Wenjing Li [a], Kaini Liang [a], Baixue Tang [b], Junyang Li [a], Jianwei Wang [b], Xiaoyu Zhu [c,**], Yanan Du [a,*]

[a] Department of Biomedical Engineering, School of Medicine, Tsinghua-Peking, Center for Life Sciences, Tsinghua University, Beijing, 100084, China
[b] School of Pharmaceutical Sciences, Tsinghua University, Beijing, 100084, China
[c] Department of Hematology, The First Affiliated Hospital of USTC, Division of Life Sciences and Medicine, University of Science and Technology of China, Hefei, China

ARTICLE INFO

Keywords:
Hematopoietic syndrome of acute radiation syndrome
Bone marrow
Hematopoietic stem cells
Mesenchymal stem cells
3D microscaffolds

ABSTRACT

Hematopoietic syndrome of acute radiation syndrome (h-ARS) is an acute illness resulted from the damage of bone marrow (BM) microenvironment after exposure to radiation. Currently, the clinical management of h-ARS is limited to medication-assisted treatment, while there is still no specific therapy for the hematopoietic injury from high-dose radiation exposure. Our study aimed to assemble biomimetic three-dimensional (3D) BM microniches by co-culture of hematopoietic stem and progenitor cells (HSPCs) and mesenchymal stem cells (MSCs) in porous, injectable and viscoelastic microscaffolds *in vitro*. The biodegradable BM microniches were then transplanted *in vivo* into the BM cavity for the treatment of h-ARS. We demonstrated that the maintenance of HSPCs was prolonged by co-culture with MSCs in the porous 3D microscaffolds with 84 μm in pore diameter and 11.2 kPa in Young's modulus compared with 2D co-culture system. Besides, the minimal effective dose and therapeutic effects of the BM microniches were investigated on a murine model of h-ARS, which showed that the intramedullary cavity-injected BM microniches could adequately promote hematopoietic reconstitution and mitigate death from acute lethal radiation with a dose as low as 1000 HSPCs. Furthermore, the mRNA expression of *Notch1* and its downstream target gene *Hes1* of HSPCs were increased when co-cultured with MSCs, while the *Jagged1* expression of the co-cultured MSCs was upregulated, indicating the significance of Notch signaling pathway in maintenance of HSPCs. Collectively, our findings provide evidence that biomimetic and injectable 3D BM microniches could maintain HSPCs, promote hematopoiesis regeneration and alleviate post-radiation injury, which provides a promising approach to renovate conventional HSPCs transplantation for clinical treatment of blood and immune disorders.

1. Introduction

Hematopoietic syndrome of acute radiation syndrome (h-ARS) comprises the damage of bone marrow (BM) microenvironment caused by accidental exposure to single high-dose radiation in a short period, which is accompanied with a myriad of serious symptoms such as BM regeneration disorder, thrombocytopenia and neutropenia, thus leads to high risk of bleeding, infection and death [1]. Moreover, radiation-induced hematopoietic system damage is not only consorted with hematopoietic stem cells (HSCs) cytotoxicity and stem cell loss [2], but also causes BM stromal cell injury [3]. Recent studies have reported that various pharmacologic agents, including antioxidants, growth factors, and anti-apoptotic agents [4–6], are used as radio-mitigators to improve the viability of hematopoietic cells both directly and indirectly. Clinically, multiple drugs such as platelets, thrombin and immunomodulators have been used in the treatment of h-ARS. However, most of them only ameliorate low radiation damage, and the protection for high-dose radiation remains underwhelming. Thus, a potent therapeutic

Peer review under responsibility of KeAi Communications Co., Ltd.
* Corresponding author.
** Corresponding author.
E-mail addresses: xiaoyuz@ustc.edu.cn (X. Zhu), duyanan@tsinghua.edu.cn (Y. Du).

https://doi.org/10.1016/j.bioactmat.2022.10.015
Received 26 July 2022; Received in revised form 26 September 2022; Accepted 12 October 2022

approach to repair or regenerate the injured HSCs microenvironment caused by radiation becomes a prerequisite for the treatment of h-ARS.

Cellular therapy, especially stem cell therapy, has emerged as a promising approach in treating h-ARS [7]. Specifically, HSCs transplantation is appraised to be an effective method for the treatment of h-ARS caused by high-dose radiation [8]. Nevertheless, the impoverished *in vitro* culture conditions, human leukocyte antigen (HLA) matching difficulty, and insufficient number of functional HSCs lead to delayed transplantation and high risk of transplantation failure, which become backdrops for broader applications [9]. Meanwhile, the difficulties in maintaining the stemness of HSCs during *in vitro* culture have been widely acknowledged, given that HSCs differentiate and lose their self-renewing potential rapidly [10]. Thus far, the majority of HSCs cultures were conducted in suspension based on the conventional two-dimensional (2D) cell culture systems [11–13], usually the planar polystyrene surface, which is incompatible with the natural BM microenvironment in regards to local micro-structures (e.g., Young's modulus and pore size). Natural BM exhibits a porous 3D structure, which possesses unique physical and mechanical characteristics with a stiffness (Young's Modulus) of 0.3–65 kPa and an internal pore size of 20–100 μm [14,15]. The local BM microenvironment which comprised of extracellular matrix (ECM) networks with multifaceted physical characteristics exerts important regulatory roles on HSCs [15]. In recent years, multiple studies have proved that 3D culture environments, such as PDMS-based bone marrow-on-a-chip [16], zwitterionic hydrogel [17], and polyethylene glycol (PEG) hydrogel [18], are more efficacious in maintaining the HSCs or hematopoietic stem and progenitor cells (HSPCs) compared with the 2D counterparts. Notwithstanding that these engineering systems have demonstrated their beneficial effects in HSCs or HSPCs culture, most systems are either too complicated or involving unfriendly process to HSPCs, which hinder their clinical applications. Despite the unique 3D and porous structure, natural BM niche encompasses versatile supporting cells, such as MSCs, adipocytes, osteocytes, and endothelial cells which contribute to the maintenance of HSCs and HSPCs [19]. HSPCs and MSCs are the major stem cell sources for cell-based therapy that have shown good efficacy in ameliorating h-ARS [20]. MSCs niche supports hematopoiesis in the BM while facilitate HSPCs proliferation under allogeneic microenvironments [21]. Therefore, based on the biomimetic 3D microscaffolds system, we devised a bionic BM *in vitro* by additionally introducing MSCs as supporting cells, thus explored the regulatory role of MSCs on HSPCs in a 3D culture system, as well as the efficacy of hematopoietic reconstruction after BM niche transplantation.

Generally, most clinical outcomes of cell therapies are unsatisfied due to the impaired migration and homing abilities, as well as the deficient functionality of transplanted cells. Previous reports demonstrated that major stem cells were entrapped in other tissues, mainly in the lungs after intravenous administration, thus led to inadequate therapeutic outcomes [22,23]. The long-term hematopoietic functions of transplanted HSPCs were facilitated by their rapid settlement in BM cavity, self-renewal and differentiation into blood lineage cells [24–26]. However, the standard delivery mode of HSPCs transplantation is intravenous infusion and the intravenously infused HSPCs will be trapped in non-hematopoietic organs and differentiate rapidly, causing unsustainable stemness and hematopoietic function [27]. Alternatively, intramedullary injection has been proven to be the most effective approach in allogeneic BM transplantation when only limited number of hematopoietic progenitors from donors are available [28]. Therefore, we envisaged the delivery of 3D biomimetic BM microniches with low-dosage of HSPCs combined with supporting MSCs to the bone cavity through intramedullary injection, thereby investigated their effects in reducing the mortality of lethal dose irradiation and improving blood reconstruction.

Here, by mimicking the structural and mechanical properties (i.e., pore size and stiffness) of natural BM microenvironment, we developed biomimetic microscaffolds with adjustable matrix stiffness and pore size which recapitulate the natural BM ECM. Furthermore, we optimized the injectability and degradability of BM microniches and integrated them into microscaffold array chip which were more accessible to cell inoculation, culture and transplantation. Based on the biomimetic microscaffolds, we provided microniches co-culture system of HSPCs and MSCs to allow the injection of the intact microniches reminiscent of BM tissues, thus maintained the cell viability and multi-cell interaction. In subsequent *in vivo* validation, the microniches constructed *in vitro* were delivered to the BM cavity as a whole to reconstruct the blood system of lethal dose irradiated mice and then promote hematopoietic reconstitution. Last, we developed a 3D microenvironment containing the minimum effective dose of HSPCs in treating severe h-ARS (Fig. 1).

2. Methods

2.1. Preparation of 3D microscaffold array chip

In order to provide a platform for the fabrication of HSPCs microniches *in vitro*, we designed the microscaffold array chips, which can be customized to different specifications such as commercial 24 well plates. Briefly, laser engraving machine was used to carve a 0.5 mm thick poly (methyl methacrylate) (PMMA) plate as the material template plate, as well as a 5 mm thick PMMA plate as the medium storage plate. The material template plate and medium storage plate were rinsed and dried with absolute ethanol and deionized water, and then hydrophilic treatment was carried out with a plasma cleaner. The preparation of gelatin-based porous microscaffolds by cryogelation was modified based on the established method [29]. 6% w/v bovine bone derived gelatin (Sigma-Aldrich, Cas. 9000-70-8) precursor solution was prepared with gelatin powder dissolved in 2% sodium 2-morpholine ethanesulfonate with pH 7.0. And then, the gelatin precursor solution was mixed with 0.1% EDC (1-ethyl-3-(3-dimethylaminopropyl) carbodiimide hydrochloride) (Aladdin) by equal volume. Then, the pre-mixed solution was applied evenly on the material template plate and placed in −20 °C refrigerator for cryogelation for 72 h. After that, the material template plate was immersed and washed in deionized water at room temperature to remove the additional crosslinking agent. The well-cleaned microscaffolds were collected and placed in −20 °C for 2 h then lyophilized for 4 h. Finally, the material template plate containing the microscaffolds were pasted and tightly assembled with the medium storage plate, which were sterilized by ultraviolet light before cell culture and implantation.

2.2. Pore size determined by SEM

After the 3D porous gelatin microscaffolds were prepared, the pore size parameters were characterized by SEM according to our previous study [29]. Briefly, three pieces of scaffolds were cut from the origin microscaffolds in random location. High-resolution images of these slices were acquired by SEM and three images were recorded for each piece of scaffold. The long and short axes of each pore were measured by ImageJ and the average diameter of that pore was counted.

2.3. Local stiffness measurement by atomic force microscope (AFM)

To characterize the local stiffness of 3D porous gelatin microscaffolds, AFM was used for measurement according to our previous study [29]. Briefly, the microscaffolds were broken into debris (less than $80 \times 80\ \mu m^2$) by the grinder to observe the single-layered wall under the microscope. After that, the microscaffolds debris were attached to the cover glass for AFM testing. Before the test, the probe was fixed with a 3 μm radius ball at the end of the AFM. During the test, the tip approached the fragment at a speed of 10 μm/s until the ball reached the debris, and a force of more than 1.5 pN was generated between the ball and the debris to complete a single test of local stiffness. At the same time, the force-displacement curve in the whole process was recorded, and the

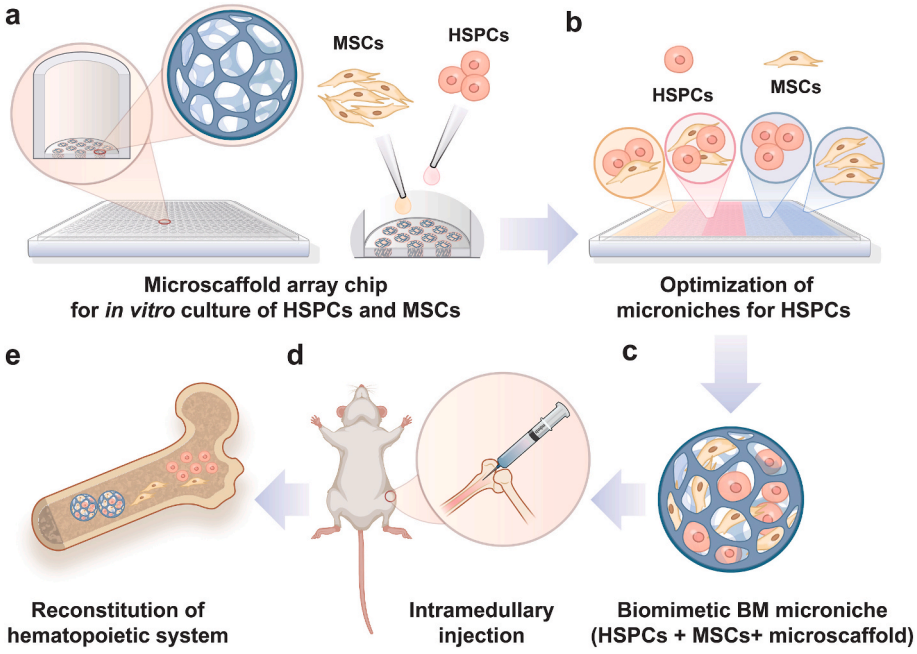

Fig. 1. Schematic representation for the construction of microscaffold array chip, co-culture of HSPCs and MSCs *in vitro*, and the therapeutic strategies for h-ARS. (a) Biomimetic microscaffold array chip with adjustable matrix stiffness and pore size similar to BM extracellular matrix was constructed. (b) Primary HSPCs and MSCs were isolated from BM of mice and were co-cultured with varied ratios in the microscaffold array chip. (c) Biomimetic BM microniches composed of HSPCs, MSCs and microscaffolds were generated. (d) Last, microniches were collected and delivered into bone marrow cavity as a whole to ameliorate irradiation damage and promote blood regeneration.

local Young's Modulus of the debris was calculated.

2.4. Mechanical characterization

Rheology measurements were made with Anton Paar RheoCompass MCR301 Rheometer mechanical tester according to the previously published method [30]. Briefly, the scaffolds were prepared in plate with 1 mm-thick and 25 mm-diameter and the tester type are PP25. Mechanical properties were then measured over time until the storage modulus reached equilibrium values. The storage modulus was periodically recorded at 10% strain and 1 Hz for 20 min. For these measurements, scaffolds were not pre-stressed.

2.5. Characterization of microscaffolds degradation and injectability

For characterization of degradation, the freeze-dried microscaffolds with consistent quality were formed and incubated in culture media with or without cells by using transwell plate at 37 °C for 3 or 6 days. Nondegradable (non-injectable) freeze-dried microscaffolds were used as control. After that, the degradable and nondegradable microscaffolds were removed from the culture medium, frozen, and then lyophilized. The dry mass of the microscaffolds was then measured after freeze-drying. The microscaffolds were injected through a 23-gauge needle to verify the injectability.

2.6. Animal study

Female or male C57BL/6-SJL (CD45.1) and C57BL/6 (CD45.2) mice were bred and maintained in the Animal Center of Tsinghua University under specific pathogen-free conditions. All mice were maintained under standard conditions on the C57BL/6 background. All animal experiments were kept to a strict protocol approved by the Animal Ethics Committee of the center of Biomedical Analysis (Institutional Animal Care and Use Committee), Tsinghua University, which is accredited by Association for Assessment and Accreditation of Laboratory Animal Care International. In all experiments, mice were randomly divided into three to five groups, and no animals or samples were excluded from the study.

2.7. Isolation and characterization of mouse BM-derived MSCs

BM-derived MSCs were isolated from C57BL/6-SJL (CD45.1) mice based on adherent culture as published previously [31]. Briefly, BM was harvested from the tibia and femur in a hood using proper sterile technique. The cell suspension was filtered through a 40 μm cell strainer to remove any bone spicules or muscle as well as cell clumps, which was further centrifuged at 500 g for 10 min at 4 °C. After centrifugation, cell suspension was suspended in Dulbecco's Modified Eagle's medium (DMEM; Sigma, St. Louis) with 1% 1 × penicillin/Streptomycin and 10% FBS (Sigma, St. Louis) and cells density was 2.5×10^7 cells/mL in 95-mm culture dishes. The plates were incubated at 37 °C with 5% CO_2 in a humidified chamber. Thereafter, the nonadherent cells were removed by changing the medium after 3 h attachment culture. After 8 h of culture, the medium was replaced with fresh complete medium. And then, the medium was changed every 2 days, and the MSCs were harvested at 80% confluence using 0.25% TrypLE™. MSCs expanded to passage four were used for cell identification, cell therapy and co-culture studies. MSCs were identified by morphology and cell surface marker. For surface marker expression, 1×10^5 MSCs were collected and the surface marker antibodies against CD44-FITC (BD Biosciences, California) and CD45-APC (BioLegend, California) were added and incubated for 30 min on the ice in the dark. The cells were washed using Hanks' Balanced Salt Solution (HBSS) with 1% 1 × penicillin/streptomycin (PS) and 10% FBS and analyzed by FACS Fortessa flow cytometer (BD Biosciences).

2.8. Sorting of BM HSPCs

HSPCs ($Lin^-c\text{-}Kit^+Sca\text{-}1^+$) from C57BL/6-SJL (CD45.1) mice (12 week-old) BM were isolated by BD Influx (BD Biosciences) as previously described [32]. Briefly, BM cells from tibiae, femurs, and pelvis were filtered through a 40 μm cell strainer. BM cells were stained with c-Kit-APC followed by magnetic bead enrichment (Miltenyi Biotec). Then, the cell suspension was stained with lineage markers of Gr-1, CD11b, Ter-119, B220, CD3, and CD4 (BioLegend, California) on the ice in the dark for 30 min. After washing the stained cells by HBSS with 1% 1 × penicillin/streptomycin and 10% FBS, the cell suspension was stained with combinations of antibodies against the following surface markers: Sca-1, c-Kit, CD150 and CD34 (BioLegend, California). The

antibodies used are listed in Supplemental Table 1. 4′,6-diamidino-2-phenylindole (Sigma-Aldrich, D8417) was used to exclude dead cells. HSPCs were sorted into Iscove's Modified Dulbecco's Medium (IMDM) supplemented with 10% FBS (Hyclone), 1% PS, and the following cytokines: murine stem cell factor (30 ng/mL), murine TPO (20 ng/mL), murine Flt-3 ligand (50 ng/mL). Thereafter, HSPCs were kept on ice for co-culturing with MSCs in the microscaffolds.

2.9. Co-culture of HSPCs and MSCs in the microscaffolds

BM-derived HSPCs and MSCs were co-cultured in 3D porous microscaffold array chip. Briefly, the prepared suspension of HSPCs and MSCs were added to the surface of the sterilized porous microscaffolds, and the cell suspension could be automatically sucked into the pores of the dried microscaffolds due to the spongy-like internal porous structure. MSCs were maintained at 10,000 cells/microniche and HSPCs density ranged from 250 to 2000 per microniche during the *in vitro* culture. After cell seeding, the microniches were incubated for 1 h at 37 °C and 5% CO_2. Thereafter, 0.6 ml per well of IMDM supplemented with 10% FBS (Hyclone), 1% PS, and the following cytokines: murine stem cell factor (30 ng/mL), murine TPO (20 ng/mL), murine Flt-3 ligand (50 ng/mL), was added to the array chip. The medium was changed every 3 days.

2.10. Scanning electron microscopy (SEM)

For SEM sample pretreatment, the microniches with cells were washed with PBS and fixed in 4% PFA for 3 h at room temperature. And then the samples were exchanged with 50%, 75%, 100% ethanol, and 100% tertiary butanol, followed by critical point dried (BAL-Tec CPD030, Leica, Wetzlar, Germany). Before coating the samples with gold, dried samples were cut using tweezers and a scalpel and orientated in the cross-sectional area. Subsequently, the samples were transferred to a vacuum chamber and sputtered with a 10 nm thin layer of gold (60 s at 30 kV, BALTec MED020, Leica). Afterwards, samples coated with gold were imaged using an Ultra 55 scanning electron microscope (Zeiss, Göttingen, Germany).

2.11. Confocal microscopy imaging

The live/dead staining by Confocal Microscopy was adopted to observe the cell growth and activity in the microscaffolds. The microniches with cells were stained with Calcein AM/PI (Abcam, Cambridge, Massachusetts) for 20 min at 37 °C. After that, the activity of HSPCs co-cultured with MSCs was confirmed by using a Zeiss LSM 700 Inverted Confocal Microscope (Zeiss, Germany). The image data were analyzed using the software of Zeiss.

2.12. Flow cytometry

After one week of culture, the cells were extracted from the microscaffolds and subsequently analyzed by flow cytometry. Specifically, the original medium was removed and 5 mg/mL type IV collagenase was added to the chip wells for 25 min at 37 °C. The digestion solution was collected until the microscaffolds were completely degraded, and the total number of cells in each group were counted by cell counter. After that, the cell suspension was washed by PBS twice and centrifuged at 500×*g* for 5 min at 4 °C. And then, the lineage antibody mixture was added for 30 min on ice followed by buffer washing. Thereafter, cells were re-suspended with antibody mix (i.e., anti-c-Kit, anti-Sca-1, anti-CD150, anti-CD48, and streptavidin) for 45 min on ice. Cells were then diluted with DAPI solution to indicate cell activity and analyzed by LSR fortessa (BD) flow cytometry.

2.13. Quantitative real-time PCR analysis

Isolation of total mRNA was carried out using TRIzol reagent (R401-01, Vazyme) after one week of culture. cDNA was prepared using reverse transcriptase (R222-01, Vazyme) according to the manufacturers' instructions. Real-time PCR was performed using AceQ qPCR SYBR Green Master Mix (Q121-02, Vazyme) on a CFX96 instrument (Bio-Rad). Relative expression levels were calculated by comparative CT method ($2^{-\triangle\triangle CT}$ method). All genes were normalized to the mRNA level of glyceraldehyde-3-phosphate dehydrogenase (GAPDH). Primers are listed in Supplemental Table 1.

2.14. Monitoring the distribution of donor cells

To monitor the transplanted microniches, engineered-MSCs that stably express luciferase by lentiviral virus-mediated gene transfer (MSCs-Akaluc) were used to verify the engraftment efficiency as previously described [33]. The template of pcDNA3-Venus-Akaluc was obtained from Atushi Miyawaki. the Akaluc sequence was cloned into lentivirus mammalian expression vector pLV-CMV-puro empty plasmid with a CMV promoter. For lentivirus production, a lentiviral expression vector was cotransfected with second-generation lentivirus packaging vectors pVSVG and pΔ8.9 into 293FT cells using Neofect (Neofect biotech). 72 h after transfection, supernatant was collected and centrifuged with 19,500 rpm for 2.5 h. Pellets were resuspended by Opti-MEM medium to a total volume of 200 μL. MSCs were seeded in 6-well plate and transfected at an MOI of 10 with the resuspended Akaluc lentivirus, along with polybrene (8 μg/mL) to assist the viral infection. After 100% confluence was reached, the cell passaging was conducted. 24 h after infection, puromycin was added to a final concentration of 2.5 μg/mL for selection. Briefly, injectable microscaffolds loaded with 2×10^4 and 2×10^5 MSCs-Akaluc were suspended in 50 μL PBS, and then the microniches were intramedullary injected into the tibiae under the sodium pentobarbital-anesthetized condition. After that, mice were intraperitoneally injected with 100 μL of TokeOni (15 mg/mL, Sigma-Aldrich) and imaged using an IVIS Lumina II imaging system (Caliper Life Sciences) to observe the distribution of MSCs *in vivo*.

In order to realize *in vivo* imaging, HSPCs were stained with DiR and MSCs were stained with DiD prior into the transplantation to the mice tibiae. The engraftment of cells was daily imaged using an IVIS Lumina II imaging system (Caliper Life Sciences). Three days after transplantation, the mice were sacrificed, and the peripheral blood cell and BM cell were collected and analyzed by flow cytometry.

2.15. Transplantation of microniches in recipient mice

Male C57BL/6 (CD45.2) mice (12 week-old) as recipient mice were housed in a specific-pathogen-free facility. At 10–12 weeks of age, mice were irradiated at a lethal dose of radiation (9 Gy) using an X-ray irradiator (RS-2000, Rad Source Technologies) before cell transplantation. Intramedullary injection was conducted as previously published with modification [34]. Specifically, the sorted cells (CD45.1) were maintained in 2D cultured (1000 HSPCs), 2D co-cultured (1000 HSPCs + 20, 000 MSCs per well), and 3D co-cultured (We define this group as microniche. i.e., 500 HSPCs +10,000 MSCs per microniche, 2 microniches per well) groups respectively in the 96 wells plate. The original medium was removed by PBS after 1 day culture. For 2D and 2D co-cultured group, all the cells were resuspended in 50 μL PBS for injection per mouse. For microniches group, 2 microniches were resuspended in 50 μL PBS for injection per mouse. After that, the free cells and microniches were injected into mouse tibiae under the sodium pentobarbital-anesthetized condition and the control mice were injected with equal volume of PBS in subsequent experiments. Recipient mice were administered with antibiotic water for 2–3 weeks following transplantation and the mortality rate was counted. The chimerism of donor cells (including myeloid, B, and T cells) in peripheral blood was analyzed by flow cytometry at 2, 4, 6, and 8 weeks after transplantation. At the end of the experiment, the recipient mice were sacrificed. The bone marrow was collected and analyzed by flow cytometry. All flow

cytometry data were analyzed by using FlowJo software, version 9.0 (TreeStar, CA). The antibodies used to analyze peripheral blood chimerism were listed in Supplemental Table 2.

2.16. Blood cell counts

At 2, 4, 6 and 8 weeks after transplantation, mice were bled and analyzed using an Auto Hematology Analyzer BC-5000 (MINDRAY).

2.17. Statistical analysis

All data were statistically analyzed by GraphPad Prism software version 6.04 (GraphPad Software Inc., USA) and expressed as the means ± standard error of the mean (SEM). One-way ANOVA or Student t tests were performed to compare the groups and two-Way ANOVA for multiple conditions over time. P values ≤ 0.05 were considered significant. All experiments were repeated 3 times independently.

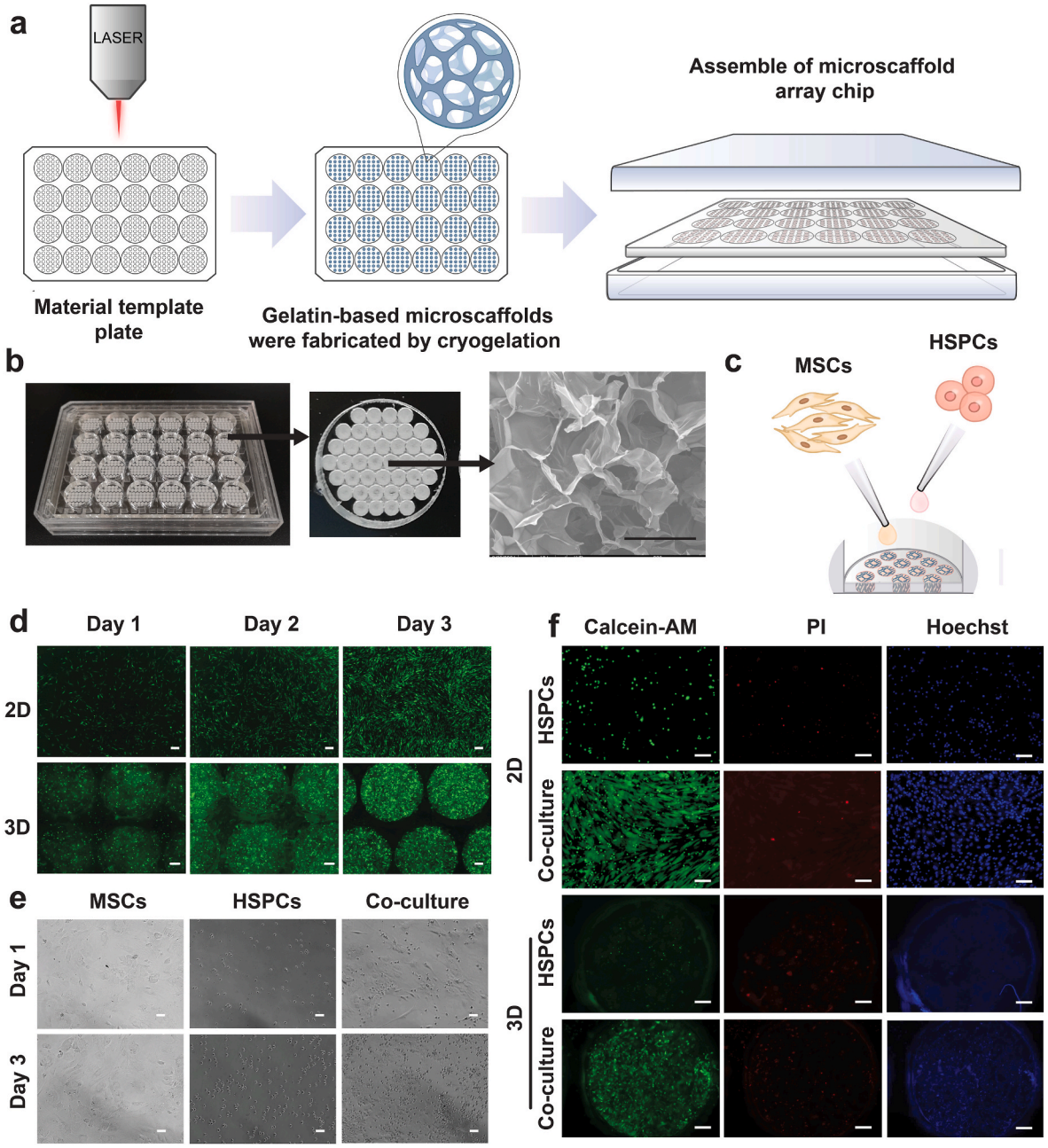

Fig. 2. Construction of microscaffold array chip for the co-culture of HSPCs and MSCs. (a) Schematic diagram of microscaffold array chip manufacturing process. Gelatin based microscaffolds were fabricated through cryogelation and finally integrated into microscaffold array chip. (b) Photo images of microscaffold array chip and SEM images of the porous microscaffolds. The white microscaffold material is 0.5 mm thick and 1.5 mm in diameter. Representative micrographs with 200 μm scale bars. (c) Schematic diagram of cells inoculation. (d) GFP^+ MSCs were seeded into the microscaffold array chip for 3 days. Representative micrographs of 2D and 3D with 100 μm and 200 μm scale bars, respectively. (e) Mono-culture of primary MSCs and co-cultured with HSPCs in the HSPCs medium for 3 days. Representative micrographs with 100 μm scale bars. (f) Live and dead characterization of HSPCs co-cultured with MSCs during the 7-day culture period. Calcein-AM stands for cells activity; PI, propidium iodide, stands for dead cells; Hoechst stands for cell nucleus. Representative micrographs of 2D and 3D with 100 μm and 200 μm scale bars, respectively.

3. Results

3.1. Construction of biomimetic microscaffold array chip for the co-culture of HSPCs and MSCs

To facilitate the study of stem cell culture *in vitro* with 3D scaffolds, we constructed a multi-well array plate with PMMA using laser engraving, which could be used as template to fabricate the gelatin microscaffolds through cryogelation (Fig. 2a). Each porous array plate contained 24 wells which were compatible to the commercial 24-well multitier plates, and the white dots in each well visualized by the naked eyes were the microscaffolds with sponge-like microstructures. Through the SEM, the interior 3D porous structure with 80–90 μm in diameter was observed (Fig. 2b). Next, we seeded green fluorescent protein (GFP+) transfected MSCs [33] into the microscaffold array chip by harnessing the spontaneous inhalation ability of freeze-dried microscaffolds, thus forming microniches to support hematopoiesis *in vitro* (Fig. 2c). We visualized GFP$^+$ MSCs inside the microscaffolds by confocal microscopy and showed that GFP$^+$ MSCs were distributed evenly in each microscaffold, and gradually proliferated in 3D microscaffold array chip (Fig. 2d and Fig. S1). Overall, the microscaffold array chip offered an efficient *in vitro* stem cell culture and characterization platform.

Next, we verified whether the microscaffold array chip was suitable for HSPCs (Lin$^-$c-Kit$^+$Sca-1$^+$) culture. Firstly, primary HSPCs were sorted by flow cytometry and were co-cultured with MSCs harvested from mouse BM (Fig. S2) for 3 days in the HSPCs medium. We found that MSCs could grow well in the HSPCs medium while HSPCs could grow stably over time in the presence of MSCs (Fig. 2e). According to the result of live/dead cell staining, we exemplified that mono-culture of HSPCs and HSPCs co-cultured with MSCs maintained good cell viability during the 7-day culture period. Interestingly, we found that HSPCs were preferentially attached to MSCs, and could not maintain their viability when cultured alone inside the microscaffolds (Fig. 2f),

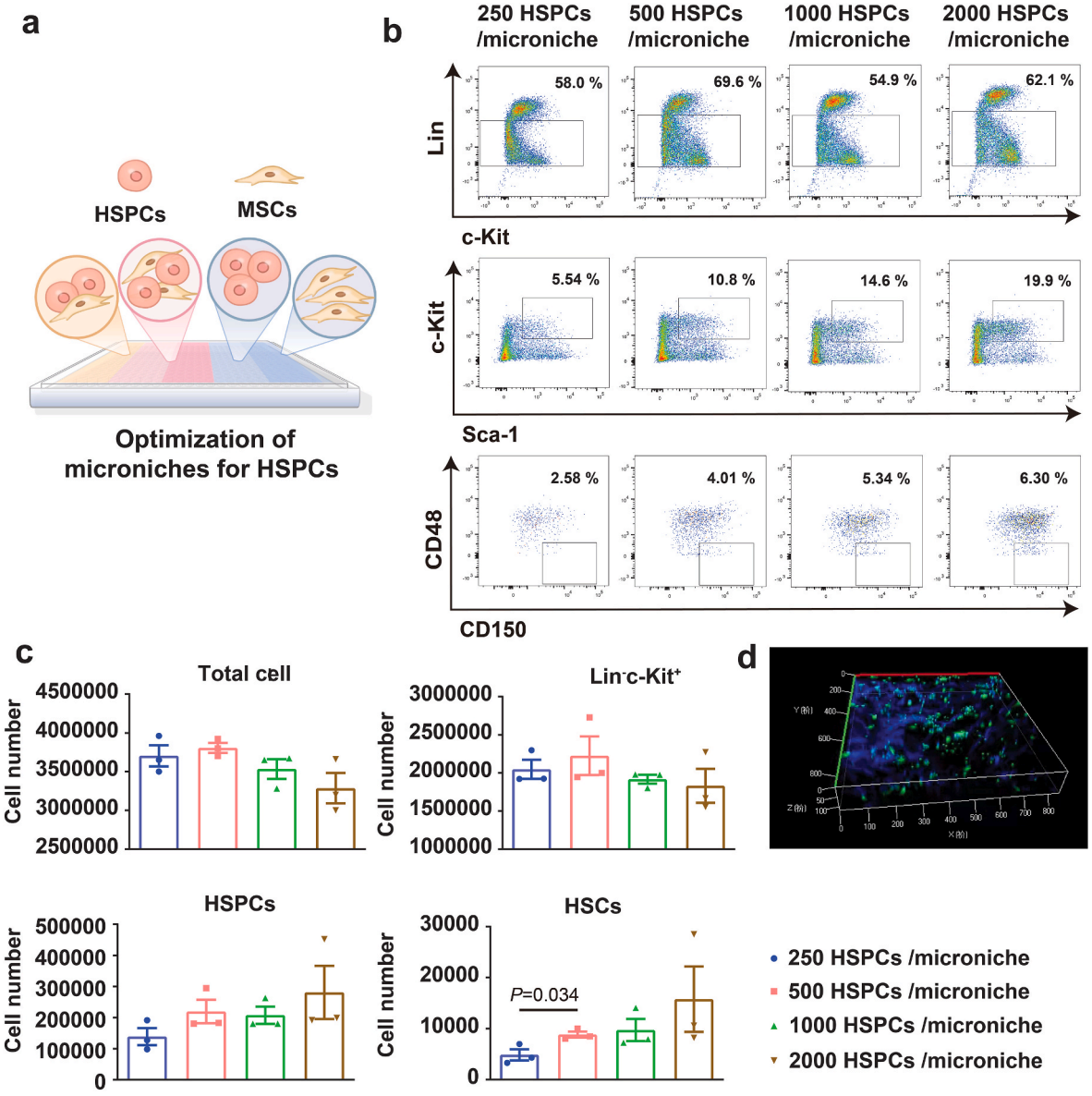

Fig. 3. Optimization of cell density for the co-culture of HSPCs and MSCs in microscaffold array chip. (a) Schematic of optimization of microniches for HSPCs. (b) Flow cytometry analysis of Lin$^-$c-Kit$^+$ cells, HSPCs (Lin$^-$c-Kit$^+$Sca-1$^+$), and HSCs (Lin$^-$c-Kit$^+$Sca-1$^+$CD150$^+$CD48$^-$) of microniches with different numbers of HSPCs inoculation. (c) Statistical analyses of flow cytometry data. (d) Characterization of microniches by 3D reconstruction imaging. Green fluorescence reflects cell viability, and blue fluorescence is originated from the autofluorescence of the microscaffolds. For all charts, data are presented as means ± SEM; data are not statistically significant when *P* values are not shown; n ≥ 3 per group.

suggesting that the support from stromal MSCs was a prerequisite for HSPCs maintenance in the 3D microscaffolds. Collectively, these results have indicated the favorable and intimate interactions between MSCs and HSPCs in the 3D porous microscaffolds.

3.2. Optimization of cell density for HSPCs

Next, we quantified the relative proliferation and maintenance of the HSPCs in the 3D microscaffolds. The initial density of HSPCs in each microniche, as well as the ratio of HSPCs and MSCs in the co-cultured system were investigated to search for the optimal conditions in maintaining HSPCs phenotypes. Both cell types were mixed and seeded in microscaffolds array simultaneously (Fig. 3a) with a fixed number of MSCs (10,000 MSCs/microniche) and varied numbers of HSPCs (250, 500, 1000, and 2000 HSPCs/microniche respectively). After 7 days, the microniches were characterized by 3D reconstruction imaging (Fig. 3d) and then the microscaffolds were digested with 5 mg/mL collagenase IV for cell collection. Lin$^-$c-Kit$^+$ cells, HSPCs (Lin$^-$c-Kit$^+$Sca-1$^+$), and HSCs (Lin$^-$c-Kit$^+$Sca-1$^+$CD150$^+$CD48$^-$) were labelled and analyzed by flow cytometry, respectively (gate methods, Fig. S3a). As shown in Fig. 3b,

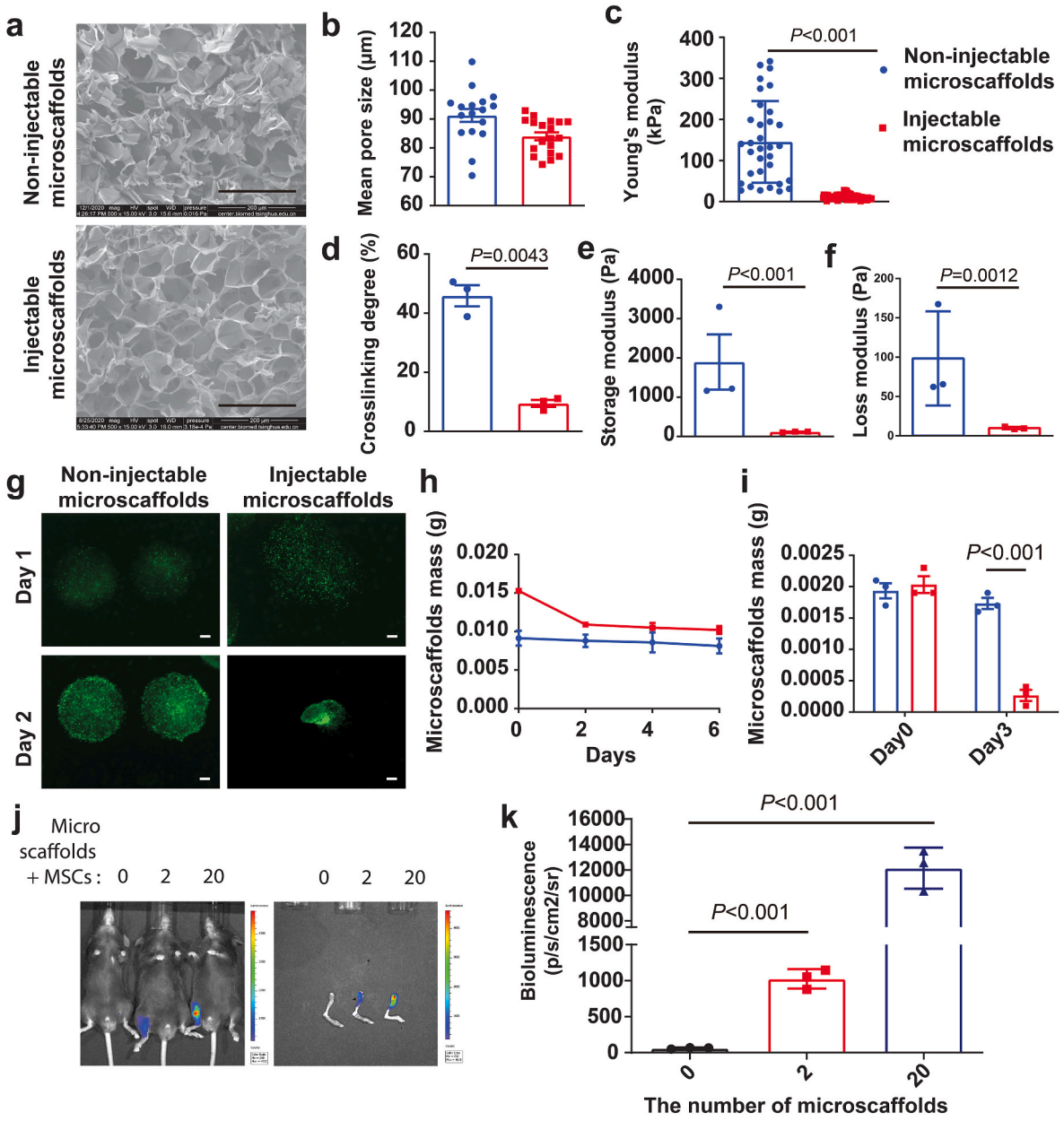

Fig. 4. Injectable and degradable viscoelastic microscaffolds for intramedullary injection. (a) Internal porous structure of non-injectable microscaffolds and injectable microscaffolds detected by SEM. Representative micrographs with 200 μm scale bars. (b) Statistical analysis of mean pore size of microscaffolds. (c) Young's modulus of microscaffolds detected by AFM. (d) Crosslinking degree of microscaffolds determined by using trinitro benzene sulfonic acid (TNBS) method. (e) Storage modulus of microscaffolds. Rheology measurements of microscaffolds were made with Rheometer mechanical tester. (f) Loss modulus of microscaffolds. (g) Fluorescence imaging of microscaffolds degradation. Representative micrographs with 200 μm scale bars. (h) Microscaffolds were incubated in culture media without cells at 37 °C for 6 days. (i) Microscaffolds were incubated in culture media with cells at 37 °C for 3 days. (j) Bioluminescence imaging for tracking cell retention based on injectable microscaffolds loaded with MSCs-Akaluc from tibia of mice in different experiment groups on days 1. (k) Measurement of the average radiance in standardized regions of luminescence signal is presented as photons per second per square centimeter per steradian (photons/s/cm^2/sr). The x-axis is the number of microscaffolds loaded with MSCs-Akaluc. For all charts, data are presented as means ± SEM; data are not statistically significant when *P* values are not shown; n ≥ 3 per group.

the proportion of Lin$^-$c-Kit$^+$ cells remained constant regardless of the initial density of HSPCs, while the ratio of HSPCs (Lin$^-$c-Kit$^+$Sca-1$^+$) and HSCs (Lin$^-$c-Kit$^+$Sca-1$^+$CD150$^+$CD48$^-$) increased proportionally with the initial seeding density. Notably, we observed that the number of HSPCs (Lin$^-$c-Kit$^+$Sca-1$^+$) and HSCs (Lin$^-$c-Kit$^+$Sca-1$^+$CD150$^+$CD48$^-$) of the 500 HSPCs/microniche group was significantly higher than that of the 250 HSPCs/microniche group while exhibited no significant difference with 1000 HSPCs/microniche group (Fig. 3d), indicating that the 500 HSPCs/microniche might contribute to the maintenance of HSPCs and thus act as a desirable initial inoculation density to construct the microniches.

3.3. Optimization of injectable and degradable viscoelastic microscaffolds for intramedullary injection

We aimed to provide a microscaffold-based co-culture system for convenient and minimally invasive delivery of a biomimetic BM microniches construct *in vivo*, without disrupting the cellular viability and multi-cellular interactions during the process of transplantation. Therefore, we optimized the Young's modulus, mechanical properties (e.g., viscoelasticity), degradability and injectability of the microscaffolds to meet the requirements of intramedullary injection, thereby directly promoted HSCs homing and colonization to the BM. In accordance with the Young's modulus (0.3–65 kPa) and internal pore size (20–100 μm) of natural BM structure [14,15], the Young's modulus and internal pore size of the microscaffolds were 11.2 kPa and 84 μm, respectively (Fig. 4a, b, c). We observed that the crosslinking degree (45.8% vs. 9.5%), the storage modulus (1.94 kPa vs. 0.12 kPa), and the loss modulus (98.4 Pa vs. 9.87 Pa) of injectable microscaffolds were significantly lower than that of non-injectable microscaffolds (Fig. 4d, e, f). The injectable microscaffolds could be delivered as whole *in vivo* by using a 23G needle through intramedullary injection (Supplementary video). In terms of degradation performance, the optimized microscaffolds could be entirely degraded in the presence of cells (Fig. 4g). Interestingly, the microscaffolds loaded with cells (HSPCs co-cultured with MSCs) were almost degraded on day 3, while the void

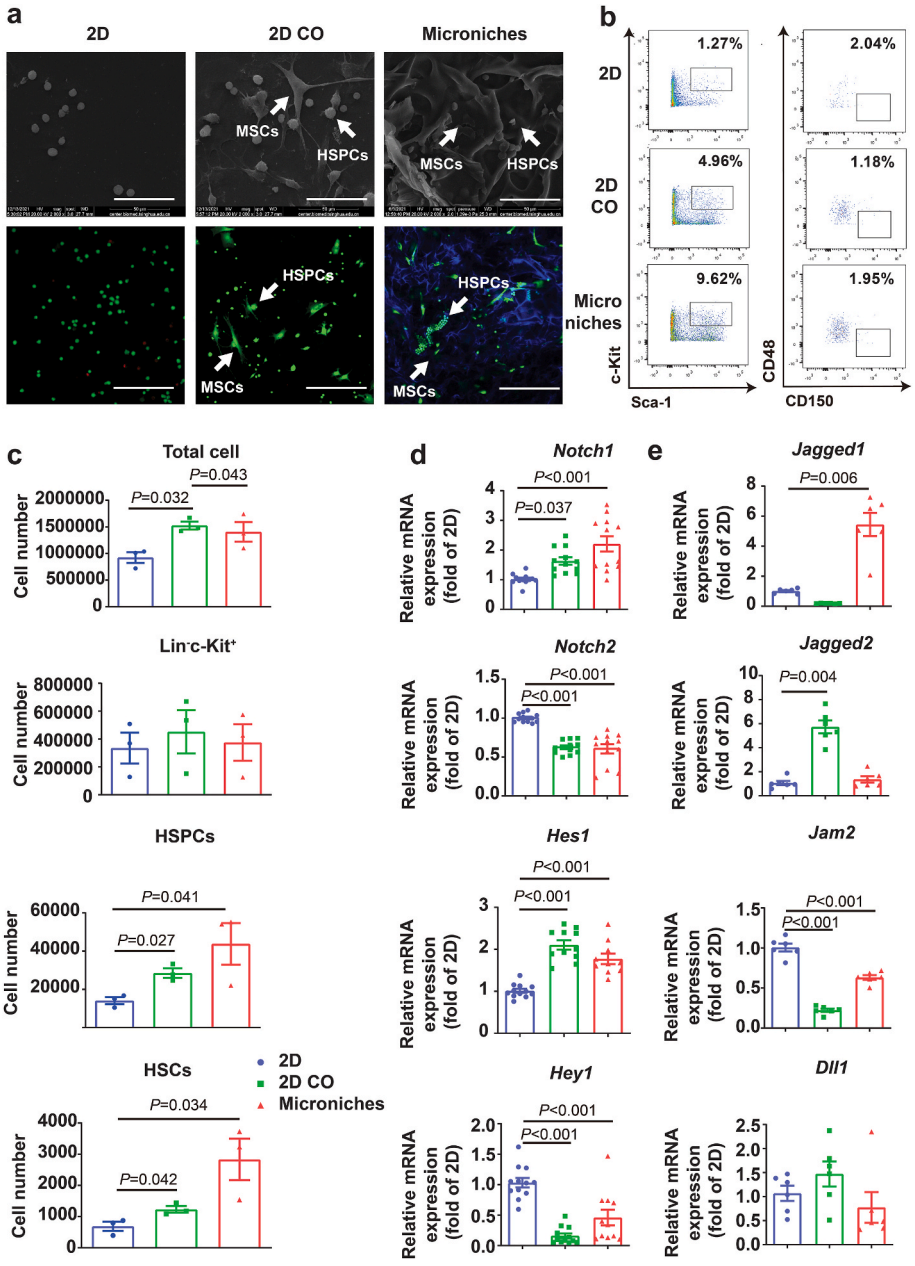

Fig. 5. Characterization of the microniches *in vitro* before intramedullary injection. (a) Internal distribution and cell activity of HSPCs and co-cultured MSCs in microniches were imaged using SEM and confocal microscopy. Representative micrographs of SEM and confocal with 200 μm and 100 μm scale bars. Green stands for cells viability and red stands for dead cells (b) Flow cytometry analysis of Lin$^-$c-Kit$^+$ cells, HSPCs (Lin$^-$c-Kit$^+$Sca-1$^+$), and HSCs (Lin$^-$c-Kit$^+$Sca-1$^+$CD150$^+$CD48$^-$) of microniches before transplantation. (c) Statistical analyses of flow cytometry data. (d) Real-time quantitative PCR was used to detect the mRNA expression of Notch-associated genes such as *Notch1*, *Notch2*, *Hes1* and *Hey1* of HSPCs. (e) Detection of the mRNA expression of Notch-ligand genes such as *Jagged1*, *Jagged2*, *Jam2* and *Dll1* of MSCs. For all charts, data are presented as means ± SEM; data are not statistically significant when *P* values are not shown; n ≥ 3 per group.

microscaffolds remained intact (Fig. 4h and i). The above data shows that we obtained injectable, degradable and viscoelastic microscaffolds to meet the demands of subsequent BM transplantation. To verify the feasibility of direct *in situ* transplantation of the biomimetic microniches with minimally invasive surgery, we leveraged Akaluc-expressed MSCs (MSCs-Akaluc) to examine the localization and survival of the injected cells. We injected MSCs-Akaluc-loaded microscaffolds into the tibia of mice, and found that the fluorescent signal increased proportionally with the number of microscaffolds injected (Fig. 4j and k), indicating that the optimized microscaffolds were appropriate for efficient cell delivery via intra-BM injection.

Supplementary video related to this article can be found at https://doi.org/10.1016/j.bioactmat.2022.10.015

3.4. Characterization of the microniches in vitro

Prior to the intramedullary injection, we characterized the *in vitro* microniches. BM HSPCs and MSCs from 8 to 12 weeks old C57BL/6-CD45.1 mice were mixed (500 HSPCs + 10,000 MSCs/microniche), seeded into the microscaffolds, and imaged using SEM. Results showed the effective spreading of MSCs within the microscaffolds, as well as the close connection between the HSPCs and co-cultured MSCs, given that HSPCs proliferated continuously in the microscaffolds within the 7-day culture (Fig. 5a). Then, we measured the cell activity by live/dead cell staining and obtained a 3D-reconstruction of the microniches through confocal microscopy. Almost all cells remained viable and distributed uniformly within the microscaffolds on day 7 (Fig. 5a).

Next, the proliferation, phenotype preservation and differentiation of HSPCs were analyzed by flow cytometry. In accordance with the previous results, MSCs were beneficial for HSPCs proliferation in

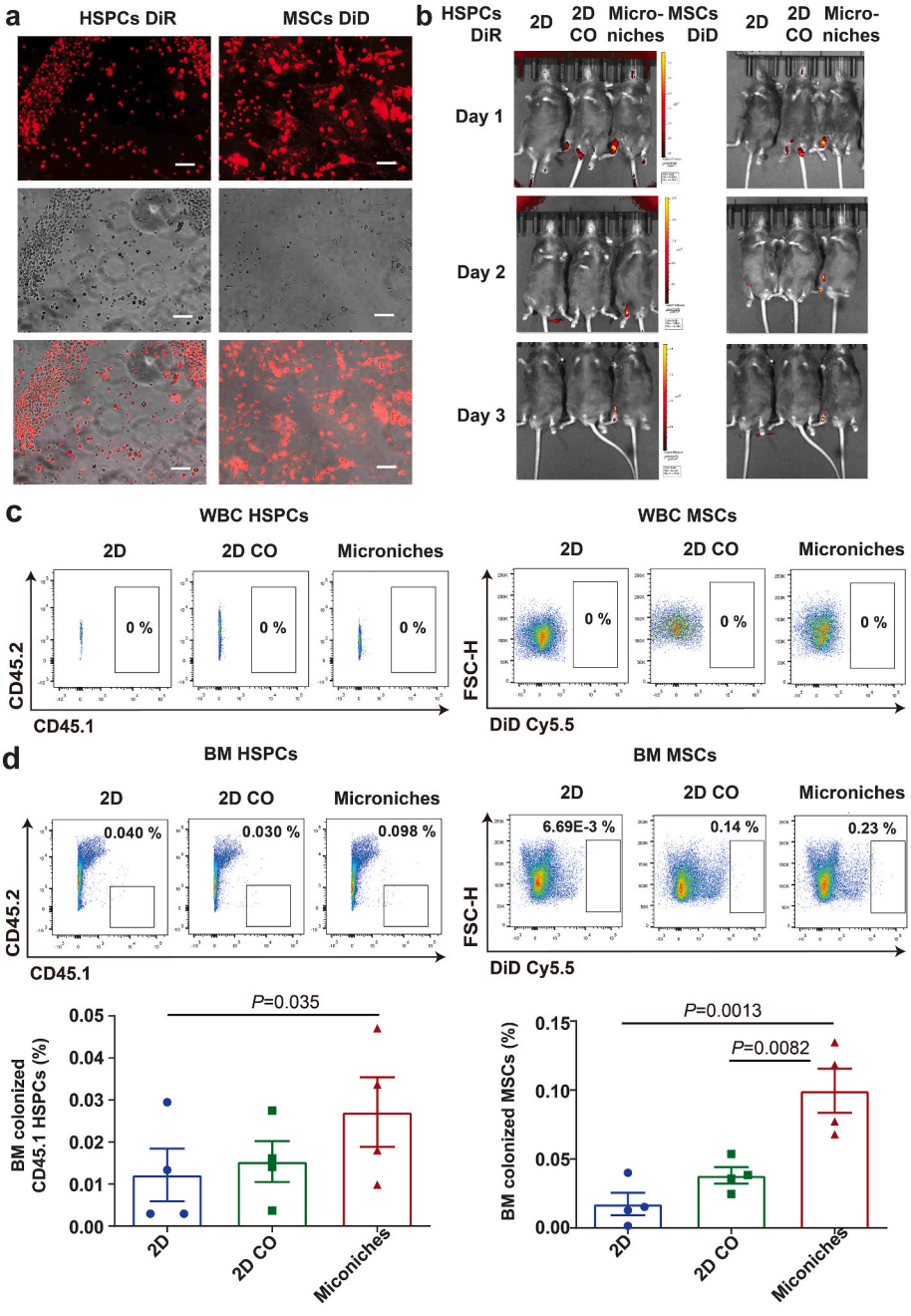

Fig. 6. Microniches promoted retention of HSPCs and MSCs in BM. (a). Fluorescent labeling imaging of HSPCs and MSCs. HSPCs were stained with DiR and MSCs were stained with DiD. Representative micrographs with 200 μm scale bars. (b) Fluorescence tracer imaging of mice after intramedullary injection of microniches from different groups for 1, 2, and 3 d (n = 4). (c) Detection of donor cells (HSPCs and MSCs) in peripheral blood by flow cytometry. No statistical analysis as donor cells were not detected in peripheral blood. WBC, whole blood cells. (d) Detection of donor cells in BM by flow cytometry. All statistical analyses are presented on the down panel of data (n = 4). BM, bone marrow. For all charts, data are presented as means ± SEM; data are not statistically significant when *P* values are not shown.

standard 2D culture, given that HSPCs co-cultured with MSCs divided 1–2 times more than HSPCs alone and showed fewer apoptotic cells under co-culture system (Fig. S4). Similarly, more HSPCs ($Lin^-c\text{-}Kit^+Sca\text{-}1^+$) and HSCs ($Lin^-c\text{-}Kit^+Sca\text{-}1^+CD150^+CD48^-$) were maintained in the presence of MSCs in the 3D microscaffolds than that in the 2D and 2D co-culture control (Fig. 5b and 5c). These results indicate the impact of the MSCs co-culture within the 3D microscaffolds on the proliferation and differentiation of HSPCs.

Given that Notch-mediated cell-to-cell signaling is involved in self-renewal, differentiation and homeostasis of HSCs and stromal cells [35], we next determined whether the interactions between HSPCs and MSCs could activate the Notch signaling pathway of HSPCs. We used real-time quantitative PCR to detect the mRNA expression of Notch-associated genes such as *Notch1*, *Notch2*, *Hes1* and *Hey1* of HSPCs. Results showed that the expression of *Notch1* and *Hes1* were greatly enhanced in the co-cultured HSPCs compared to the mono-cultured HSPCs (Fig. 5d). In addition, the expression of *Jagged1* was significantly upregulated during 3D co-culture while *Jagged2* was significantly upregulated in 2D co-culture of MSCs (Fig. 5e). Collectively, these results indicated that the 3D microniches promoted the physical contact between MSCs and HSPCs, thereby improved the maintenance of HSPCs, which may involve the activation of Notch signaling pathway.

3.5. Immunofluorescence and FACS detection of donor HSPCs injected into bone marrow cavity

In order to verify the distribution of the transplanted HSPCs *in vivo*, the fluorescent dye DiR was used to label HSPCs, while DiD was used to label MSCs (Fig. 6a). We seeded the fluorescently labelled cells into the microscaffolds for one day, and then carried out BM cavity transplantation. The distribution of cells was imaged and characterized by the small animal *in vivo* imaging system. As shown in Fig. 6b, HSPCs and MSCs in the microniche group remained colonized in the BM cavity after 3 days of injection.

The quantitative characterizations of HSPCs and MSCs in peripheral blood and BM were detected by using flow cytometry. After 3 days of transplantation, donor cells (HSPCs and MSCs) were almost undetectable in peripheral blood (Fig. 6c), while the donor cells residing in the BM of the microniches group were significantly higher than those in other groups (Fig. 6d), indicating that the microniches could promote the colonization of HSPCs and MSCs in the BM.

3.6. Intramedullary injection of microniches with low-dose HSPCs promoted peripheral blood recovery and rescued mice from severe h-ARS

We next investigated the hematopoietic support of the microniches *in vivo*, as well as the minimal effective dose of microniches which was able to rescue the lethally-irradiated mice. Firstly, 5000, 2500, 1000, and 500 HSPCs were transplanted by intravenous injection. We found that the survival rate of mice in 1000 HSPCs-transplanted group could not reach the median lethal dose (Fig. S5). Therefore, 1000 HSPCs was considered as the minimum effective dose in the intramedullary injection trial. Based on that, we cultured the HSPCs (500) isolated from the 8–12 weeks old C57BL/6-CD45.1 mouse BM and MSCs (10,000) on one microscaffold for one day. CD45.2 mice were subsequently divided into six groups, namely control (PBS), free 2D MSCs group (2D MSCs), 3D MSCs group (3D MSCs), free 2D 1000 HSPCs group (2D), free 2D co-culture cell group (2D CO), and microniches group (Fig. 7a). All mice were treated by lethal dose irradiation (9 Gy). At day 1 of *in vitro* culture, all cells were counted and shown viable before transplantation (Fig. S6). We then collected and delivered the microniches to the recipient mouse's intra-tibia (two microniches for each mouse), and the mortality rate was evaluated in the subsequent weeks. Interestingly, all mice died within 3 weeks in the PBS group and 2D group, while the co-culture groups (2D CO, microniches) showed reduced mortality. In contrast, transplantation of MSCs alone or MSCs-loaded microscaffolds could not rescue the lethally-irradiated mice (Fig. 7b). To explore the therapeutic effects of injected microniches, we analyzed the lineage differentiation of donor cells (isolated from CD45.1 mice) in the recipient CD45.2 mice by flow cytometry, which could determine the chimerism rate of donor HSPCs. As shown in Fig. S3b, CD45.1 represented the cells of donor origin and CD45.2 represented the cells from the host. The chimeric rate of HSPCs cultured in the microniches group was significantly higher than that in the 2D CO group (Fig. 7c). Besides, the B lymphocyte and megakaryocyte (MK) of the recipient mouse in the microniches group was significantly higher than that in the 2D CO group at 8 weeks and 4 weeks, respectively (Fig. 7c). Meanwhile, the tail vein blood of recipient mice was collected for blood routine analysis. The results indicated that the whole blood cells and lymphocytes of peripheral blood in the microniches group were both higher than those in the 2D CO group. Besides, the platelet reconstitution in microniches group was significantly higher than that of 2D CO group after 4-week transplantation, which was consistent with the regeneration of megakaryocyte (Fig. 7d). In accordance with the reconstruction of peripheral blood, microniches could improve the chimerism of donor HSPCs in BM (Fig. S7). Collectively, the above phenomenon suggested that the microniches exhibited supercity in promoting hematopoietic reconstruction than the 2D co-culture system.

4. Discussion

BM is the main site of continuous de novo production of all HSPCs in adults with complex mechanisms to ensure a balance between hematopoietic output and HSPCs maintenance [36,37]. It is susceptible to irradiation, which causes hematopoietic damage and inhibition which eventually leads to h-ARS. Currently, there is still no effective therapies available, and there is an urgent need to explore effective therapies.

h-ARS not only damages HSPCs, but also adversely affects the BM's stromal cell and ECM [20]. To treat h-ARS, we developed a biomimetic BM microniches *in vitro* that recapitulated the porous structure and stiffness of the natural BM matrix, orchestrated with primary HSPCs and MSCs co-culture, to replace the irradiated BM through BM cavity administration. Simultaneously, we optimized the injectability and degradability of the viscoelastic microscaffolds to fulfil the requirements of syringe-based injection and transplantation. The microfabricated array chip could be easily scaled up to produce highly elastic and porous microscaffolds.

Our system successfully recapitulated the cellular interactions at hematopoietic niche by co-culturing HSPCs and MSCs in microniches. From the *in vitro* results, we found that HSPCs cultured alone or co-cultured with MSCs maintained good cell viability under the 2D culture system, while the survival of HSPCs in 3D microscaffold array chip was dependent on the presence of the MSCs. Interestingly, more HSPCs and HSCs were maintained in the presence of MSCs in 3D microscaffolds compared to 2D and 2D co-culture control. These results indicated that the support of stromal MSCs was necessary for 3D culture of HSPCs. It is increasingly sophisticated that MSCs play a prominent role in the regulation, self-renewal and differentiation of HSPCs, which is supported by the direct cell-cell interaction at the sites of hematopoiesis [21,38]. Consistently, we delineated the role of MSCs as feeder cells on proliferation and phenotype of HSPCs. Notch-mediated cell-to-cell signaling is involved in the self-renewal, differentiation and homeostasis of hematopoietic cells [35]. Similarly, we observed the activation of Notch1 signaling and upregulated expression of Jagged1 in microniches. These results indicated that MSCs aided in the maintenance of HSCs through the activation of Notch signaling.

Homing and engraftment of HSPCs to the injury BM are vital for blood system regeneration and the cure of h-ARS. HSPCs produced from *in vitro* culture are often associated with varying degrees of dysfunction, including a decrease or loss of homing and implantability. Likewise, we found that the co-transfusion of HSPCs with MSCs promoted blood regeneration and improved survival in mice from radiation damage. In

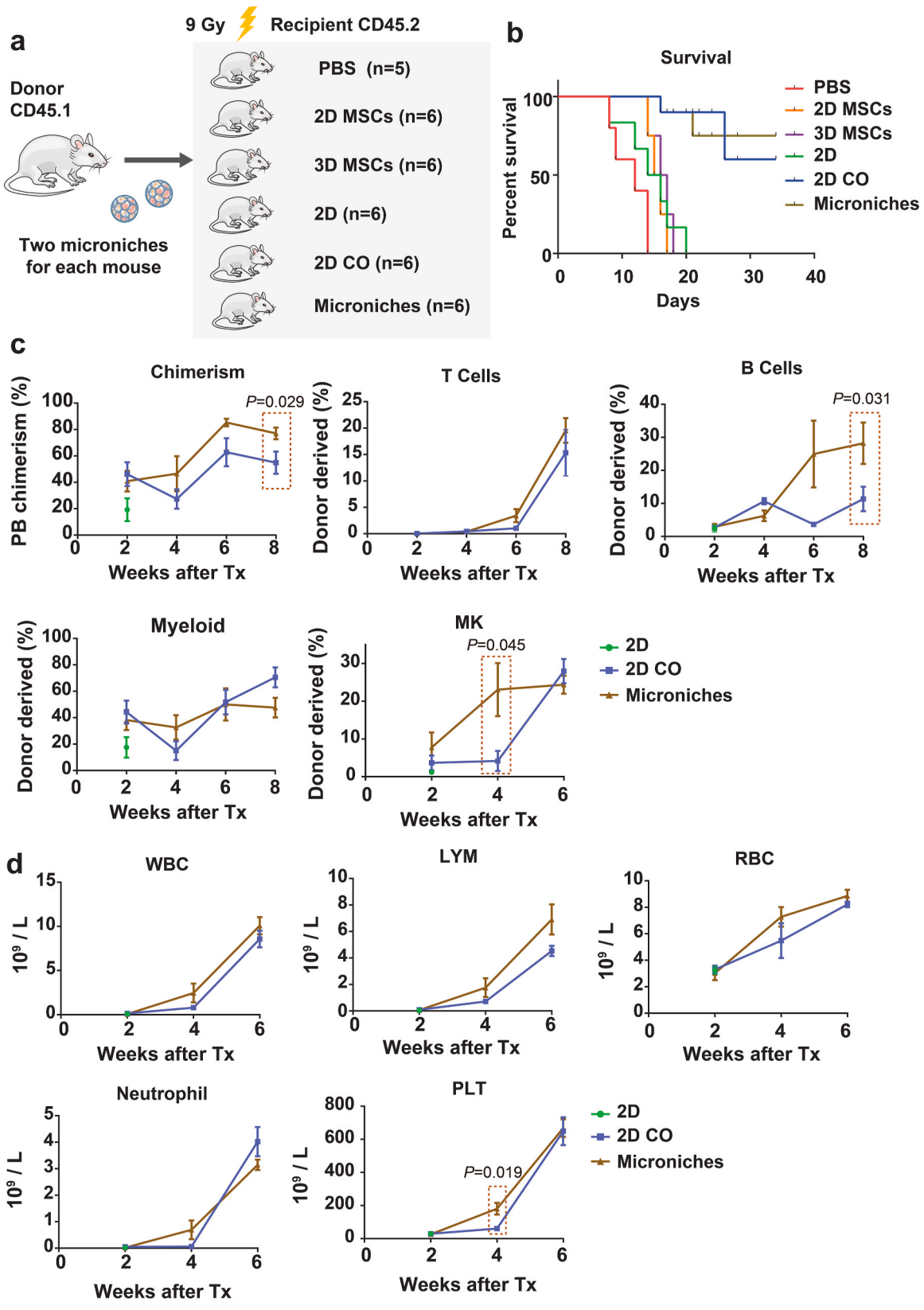

Fig. 7. Microniches with low-dose HSPCs promoted hematopoiesis regeneration. (a) Schematic of grouping and treatment of mice. CD45.1 mice as donor, CD45.2 mice as recipient were subsequently divided into six groups under 9 Gy irradiation. (b) Survival curve of mice after transplantation. (c) Flow cytometry analysis of lineage differentiation of donor cells (isolated from CD45.1 mice) in the recipient CD45.2 mice (n = 4). MK, megakaryocyte. (d) Blood routine analysis of the tail vein blood of recipient mice (n = 4). WBC, whole blood cells; LYM, lymphocyte; RBC, red blood cell; PLT, platelet. For all charts, data are presented as means ± SEM; data are not statistically significant when *P* values are not shown.

addition, the efficacy and function of HSCs transplantation are dependent on the injection method and the administration route. Previous reports have shown that intravenous infusion of stem cells caused their entrapment in the lung and liver, resulted in poor clinical outcomes [22,23]. To reconcile this major drawback, we delivered the microniches to the irradiated BM through BM cavity injection. We postulated that transplanted free cells could not accomplish efficient homing to the BM, while the injectable microniches improve the implantation of HSPCs and MSCs. Most notably, we observed the rapid regeneration of MK and platelets in recipient mice, proving the role of microniches in the rapid reconstruction of the blood system of radiation-damaged mice, especially promoted the colonization of lymphocytes and platelets.

Clinically, cord blood HSPCs transplantation not only faced the problem of slow colonization of neutrophils and platelets, but also hindered by the limited number of donor HSPCs [39,40]. Therefore, we used a mouse model to screen the lowest effective dose of HSPCs to treat lethally irradiated mice. We applied 1000 HSPCs-containing microniches and directly transplanted them to the BM cavity, which were proved to be sufficient to reduce the mortality of lethally irradiated mice. It implied that the microniches-based culture and delivery method developed in this study can potentially reduce the minimum effective dose of human cord blood $CD34^+$ HSPCs for transplantation, thus saving more irradiated patients despite of the limited cord blood supply. Meanwhile, the microniches could promote the colonization of lymphocytes and platelets in the mouse h-ARS model, which provides a promising approach to renovate conventional HSPCs transplantation for clinical treatment of blood and immune disorders.

In conclusion, *in vitro* biomimetic BM microniches could promote the maintenance of HSPCs. The intact microniches were delivered through the BM cavity, with a minimal number of hematopoietic progenitors could promote hematopoiesis regeneration and improve survival after radiation injury. The injectable microniches-based cultivation and delivery approach shows promise to advance the clinical application of cord blood HSPCs for the treatment of h-ARS as well as other blood and immune disorders.

Funding

This work was financially supported by National Natural Science Foundation of China (82125018), and the Beijing Municipal Science and Technology Commission (Z181100001818005).

Author contributions

Y.D., X.Z, and H.L. designed the research; H.L. performed experiments, analyzed and interpreted data, wrote the paper, and coordinated the project. Y.A. conducted the research and analyzed data. W.L., B.T. and K.L. prepared the figures and drafted the manuscript. J.L. performed SEM and viscoelasticity characterization of scaffolds. J.W. provided guidance on animal experiments. Y.D. provided overall intellectual guidance, edited the manuscript, and is the principal investigator of the supporting grants. All authors read and approved the final manuscript.

Data and materials availability

All data pertaining to this study are present in the paper and/or in the Supplementary Materials. Requests for other information and reagents may be directed and will be fulfilled by the corresponding author, Y.D. (duyanan@tsinghua.edu.cn).

Ethics approval and consent to participate

All animal experiments were kept to a strict protocol approved by the Animal Ethics Committee of the center of Biomedical Analysis (Institutional Animal Care and Use Committee), Tsinghua University, which is accredited by Association for Assessment and Accreditation of Laboratory Animal Care International.

Declaration of competing interest

Y.D., H.L., Y.A. and W.L. were listed as the inventors on a patent application for microniches for h-ARS therapy. The initial filing was assigned the Chinese patent application no. 2021111092098 and no. 2022101428317. All other authors declare that they have no competing interests.

Acknowledgments

We would like to acknowledge the help from all members of Y.D.'s laboratory. We thank Dr. Ye Liu for the modification of article. We thank Prof. Yan Shi from School of Medicine, Tsinghua University and Dr. Zhaozhao Wu for technical support for AFM.

Appendix A. Supplementary data

Supplementary data to this article can be found online at https://doi.org/10.1016/j.bioactmat.2022.10.015.

References

[1] F. Milano, et al., Notch-expanded murine hematopoietic stem and progenitor cells mitigate death from lethal radiation and convey immune tolerance in mismatched recipients, STEM CELLS Translational Medicine 6 (2) (2017) 566–575.
[2] P. Mauch, et al., Hematopoietic stem cell compartment: acute and late effects of radiation therapy and chemotherapy, Int. J. Radiat. Oncol. Biol. Phys. 31 (5) (1995) 1319–1339.
[3] R. Zuo, et al., BM-MSC-derived exosomes alleviate radiation-induced bone loss by restoring the function of recipient BM-MSCs and activating Wnt/beta-catenin signaling, Stem Cell Res. Ther. 10 (1) (2019) 30.
[4] L.G. Burdelya, et al., An agonist of toll-like receptor 5 has radioprotective activity in mouse and primate models, Science 320 (5873) (2008) 226–230.
[5] V.K. Singh, et al., Tocols induce G-CSF and mobilise progenitors that mitigate radiation injury, Radiat. Protect. Dosim. 162 (1–2) (2014) 83–87.
[6] L.A. Basile, et al., HemaMax, a recombinant human interleukin-12, is a potent mitigator of acute radiation injury in mice and non-human primates, PLoS One 7 (2) (2012), e30434.
[7] L. Qian, J. Cen, Hematopoietic stem cells and mesenchymal stromal cells in acute radiation syndrome, Oxid. Med. Cell. Longev. 2020 (2020), 8340756.
[8] T.M. Fliedner, et al., Stem cells, multiorgan failure in radiation emergency medical preparedness: a U.S./European Consultation Workshop, Stem Cell. 27 (5) (2009) 1205–1211.
[9] J. Mattsson, O. Ringden, R. Storb, Graft failure after allogeneic hematopoietic cell transplantation, Biol. Blood Marrow Transplant. 14 (1 Suppl 1) (2008) 165–170.
[10] L. Rodling, et al., 3D models of the hematopoietic stem cell niche under steady-state and active conditions, Sci. Rep. 7 (1) (2017) 4625.
[11] Z. Du, et al., Optimization of SCF feeding regimen for ex vivo expansion of cord blood hematopoietic stem cells, J. Biotechnol. 164 (2) (2012) 211–219.
[12] J.S. Choi, B.A. Harley, The combined influence of substrate elasticity and ligand density on the viability and biophysical properties of hematopoietic stem and progenitor cells, Biomaterials 33 (18) (2012) 4460–4468.
[13] S.S. Kumar, et al., The combined influence of substrate elasticity and surface-grafted molecules on the ex vivo expansion of hematopoietic stem and progenitor cells, Biomaterials 34 (31) (2013) 7632–7644.
[14] L.E. Jansen, et al., Mechanics of intact bone marrow, J. Mech. Behav. Biomed. Mater. 50 (2015) 299–307.
[15] A. Gomariz, et al., Quantitative spatial analysis of haematopoiesis-regulating stromal cells in the bone marrow microenvironment by 3D microscopy, Nat. Commun. 9 (1) (2018) 2532.
[16] S. Sieber, et al., Bone marrow-on-a-chip: long-term culture of human haematopoietic stem cells in a three-dimensional microfluidic environment, J Tissue Eng Regen Med 12 (2) (2018) 479–489.
[17] T. Bai, et al., Expansion of primitive human hematopoietic stem cells by culture in a zwitterionic hydrogel, Nat. Med. 25 (10) (2019) 1566–1575.
[18] U. Blache, et al., Dual role of mesenchymal stem cells allows for microvascularized bone tissue-like environments in PEG hydrogels, Adv Healthc Mater 5 (4) (2016) 489–498.
[19] T. Sakamoto, et al., Notch signaling in nestin-expressing cells in the bone marrow maintains erythropoiesis via macrophage integrity, Stem Cell. 37 (7) (2019) 924–936.
[20] S. Chinnapaka, et al., Allogeneic adipose-derived stem cells mitigate acute radiation syndrome by the rescue of damaged bone marrow cells from apoptosis, Stem Cells Transl Med 10 (7) (2021) 1095–1114.
[21] S. Crippa, et al., Role of ex vivo expanded mesenchymal stromal cells in determining hematopoietic stem cell transplantation outcome, Front. Cell Dev. Biol. 9 (2021), 663316.

[22] B. Cousin, et al., Reconstitution of lethally irradiated mice by cells isolated from adipose tissue, Biochem. Biophys. Res. Commun. 301 (4) (2003) 1016–1022.
[23] E. Eggenhofer, et al., Mesenchymal stem cells are short-lived and do not migrate beyond the lungs after intravenous infusion, Front. Immunol. 3 (2012) 297.
[24] T. Yin, L. Li, The stem cell niches in bone, J. Clin. Invest. 116 (5) (2006) 1195–1201.
[25] Z.N. Ozdemir, S. Civriz Bozdag, Graft failure after allogeneic hematopoietic stem cell transplantation, Transfus. Apher. Sci. 57 (2) (2018) 163–167.
[26] J.P. Chute, Stem cell homing, Curr. Opin. Hematol. 13 (6) (2006) 399–406.
[27] V. Chander, G. Gangenahalli, Emerging strategies for enhancing the homing of hematopoietic stem cells to the bone marrow after transplantation, Exp. Cell Res. 390 (1) (2020), 111954.
[28] S. Ikehara, A novel strategy for allogeneic stem cell transplantation: perfusion method plus intra-bone marrow injection of stem cells, Exp. Hematol. 31 (12) (2003) 1142–1146.
[29] S. Jiang, et al., Cryoprotectant enables structural control of porous scaffolds for exploration of cellular mechano-responsiveness in 3D, Nat. Commun. 10 (1) (2019) 3491.
[30] O. Chaudhuri, et al., Hydrogels with tunable stress relaxation regulate stem cell fate and activity, Nat. Mater. 15 (3) (2016) 326–334.
[31] M. Soleimani, S. Nadri, A protocol for isolation and culture of mesenchymal stem cells from mouse bone marrow, Nat. Protoc. 4 (1) (2009) 102–106.
[32] H. He, et al., Aging-induced IL27Ra signaling impairs hematopoietic stem cells, Blood 136 (2) (2020) 183–198.
[33] Y. Zhang, et al., Exendin-4 gene modification and microscaffold encapsulation promote self-persistence and antidiabetic activity of MSCs, Sci. Adv. 7 (27) (2021).
[34] Y. Li, et al., Antioxidant small molecule compound chrysin promotes the self-renewal of hematopoietic stem cells, Front. Pharmacol. 11 (2020) 399.
[35] A. Kim, et al., Mesenchymal stem cell-mediated Notch2 activation overcomes radiation-induced injury of the hematopoietic system, Sci. Rep. 8 (1) (2018) 9277.
[36] S.J. Morrison, D.T. Scadden, The bone marrow niche for haematopoietic stem cells, Nature 505 (7483) (2014) 327–334.
[37] C. Nombela-Arrieta, M.G. Manz, Quantification and three-dimensional microanatomical organization of the bone marrow, Blood Adv 1 (6) (2017) 407–416.
[38] S.C. Mendes, C. Robin, E. Dzierzak, Mesenchymal progenitor cells localize within hematopoietic sites throughout ontogeny, Development 132 (5) (2005) 1127–1136.
[39] K.A. Al-Anazi, Autologous hematopoietic stem cell transplantation for multiple myeloma without cryopreservation, Bone Marrow Res 2012 (2012), 917361.
[40] M. Remberger, et al., Effect of total nucleated and CD34(+) cell dose on outcome after allogeneic hematopoietic stem cell transplantation, Biol. Blood Marrow Transplant. 21 (5) (2015) 889–893.